SUPPLEMENTARY MATERIAL

Supplementary File 1: Radiomic feature definitions.

We analyzed ten quantitative features each from tumors segmented under T1-weighted and FLAIR imaging at baseline and six weeks follow-up. These features can broadly be categorized into 1) first-order statistics of the histogram of all voxels, 2) tumor shape features, and 3) features quantifying tumor texture. To quantify texture, we used three texture matrices that hold the number of textural patterns found in an image. To define these matrices and features that are calculated using these matrices in the following, we first define N_g to be the number of discrete gray-levels and N_p to be the number of voxels in an image. More information can be found in the Supplementary Material of Aerts et al., Nature Communications 2014 and Coroller et al., Radiotherapy & Oncology 2015.

GLCM. A Gray-Level Co-occurrence matrix (GLCM) $P(i,j;\delta,\alpha)$ of size $N_g \times N_g$ describes the second-order joint probability function of an image, where the $P(i,j)$ is the number of times the combination of intensity values i and j occur in two pixels in the image which are separated from each other by δ pixels in direction α. Furthermore, we define $\mu = mean(P(i,j))$, $p_x(i) = \sum_{j=1}^{N_g} P(i,j)$ are the marginal row probabilities, $p_y(i) = \sum_{i=1}^{N_g} P(i,j)$are the marginal column probabilities,μ_x is the mean of p_x, μ_y the mean of p_y, σ_x is the standard deviation of p_x, σ_y the standard deviation of p_y, $HX = -\sum_{i=1}^{N_g} p_x(i) \log_2[p_x(i)]$ be the entropy of p_x, $HY = -\sum_{i=1}^{N_g} p_y(i) \log_2[p_y(i)]$ be the entropy of p_y, and $H = -\sum_{i=1}^{N_g} \sum_{j=1}^{N_g} P(i,j) \log_2[P(i,j)]$ be the entropy of $P(i,j)$. Finally, $HXY1 = -\sum_{i=1}^{N_g} \sum_{j=1}^{N_g} P(i,j) \log(p_x(i)p_y(j))$, and $HXY2 = -\sum_{i=1}^{N_g} \sum_{j=1}^{N_g} p_x(i)p_y(j) \log(p_x(i)p_y(j))$. The latter denotations are required to define those textural features that use a GLCM.

RLGL. A Run-Length Gray-Level matrix (RLGL) is used to quantify gray-level runs of different lengths in an image. A gray-level run is a stretch of consecutive pixels that have the same gray-level value. In an RLGL $p(i,j|\theta)$, the (i,j)th element describes the number of times j a gray level i appears consecutively in direction θ. Furthermore, we define N_r to be the number of different run lengths in an image.

GLSZM. A Gray-Level Size-Zone Matrix (GLSZM) quantifies the number of size-zones in an image. Instead quantifying in several directions as the GLCM or RLGL, a GLSZM quantifies at flat size-zone in the entire 3D image. A flat size-zone is a group of connecting pixel with same grey level in any direction. In a GLSZM $p(i,j)$, the (i,j)th element describes the frequency of matrices of size j with gray level i. For features using a GLSZM, we define N_r to be the number of different size-zones in an image.

Supplementary Table 1: Features derived from T1-weighted imaging.

Category	**Feature**	**Description**	**Matrix**	**Formula**
Texture	Cluster Shade	Lack of symmetry of texture matrix.	GLCM	$\sum_{i=1}^{N_g}\sum_{j=1}^{N_g}\left[i+j-\mu_x(i)-\mu_y(j)\right]^3 P(i,j)$
Texture	Correlation	Linear dependency of gray-levels in neighboring pixels.	GLCM	$\frac{\sum_{i=1}^{N_g}\sum_{j=1}^{N_g} ijP(i,j)-\mu_i(i)\mu_j(j)}{\sigma_x(i)\sigma_y(j)}$
Texture	Energy	Total sum of squared texture values (i.e., signal variance).	GLCM	$\sum_{i=1}^{N_g}\sum_{j=1}^{N_g}[P(i,j)]^2$
Texture	Informational correlation 1	Standardized correlation of entropy.	GLCM	$\frac{HXY-HXY1}{\max\{HX,HY\}}$
Texture	Informational correlation 2	Exponentially weighted correlation of entropy.	GLCM	$\sqrt{1-e^{-2(HXY2-HXY)}}$
Texture	Intensity variability	Normalized energy of gray-level size-zones.	GLSZM	$\frac{\sum_{i=1}^{N_g}\left[\sum_{j=1}^{N_r} p(i,j)\right]^2}{\sum_{i=1}^{N_g}\sum_{j=1}^{N_r} p(i,j)}$
Texture	Low-intensity large-area emphasis	Quantifies gray-level size-zones with low intensity that cover a large area.	GLSZM	$\frac{\sum_{i=1}^{N_g}\sum_{j=1}^{N_r}\left[\frac{p(i,j)j^2}{i^2}\right]}{\sum_{i=1}^{N_g}\sum_{j=1}^{N_r} p(i,j)}$
Texture	Small-area emphasis	Weights small neighboring areas.	GLSZM	$\frac{\sum_{i=1}^{N_g}\sum_{j=1}^{N_r}\left[\frac{p(i,j)}{j^2}\right]}{\sum_{i=1}^{N_g}\sum_{j=1}^{N_r} p(i,j)}$
Texture	Zone Percentage	Ratio of homogenous tumor zones and the total voxel count.	GLSZM	$\sum_{i=1}^{N_g}\sum_{j=1}^{N_r}\frac{p(i,j)}{N_p}$

Supplementary Table 2: Features derived from FLAIR imaging.

Category	Feature	Description	Matrix	Formula
Texture	Max Probability	The highest number of times a combination of pixels was found.	GLCM	$\max\{P(i,j)\}$
Texture	Low-intensity small-area emphasis	Quantifies gray-level size-zones with low intensity that cover a large area	GLSZM	$\frac{\sum_{i=1}^{N_g}\sum_{j=1}^{N_r}\left[\frac{p(i,j)}{i^2 j^2}\right]}{\sum_{i=1}^{N_g}\sum_{j=1}^{N_r} p(i,j)}$
Texture	Size-zone variability	Variance in sizes of uniform zones.	GLSZM	$\frac{\sum_{j=1}^{N_r}\left[\sum_{i=1}^{N_g} p(i,j)\right]^2}{\sum_{i=1}^{N_g}\sum_{j=1}^{N_r} p(i,j)}$
Texture	Zone percentage	Ratio of homogenous tumor zones and the total pixel count.	GLSZM	$\sum_{i=1}^{N_g}\sum_{j=1}^{N_r}\frac{p(i,j)}{N_p}$
Texture	Low-gray level-run emphasis	Quantifies number consecutive stretches of low gray-levels in the texture matrix of the image	RLGL	$\frac{\sum_{i=1}^{N_g}\sum_{j=1}^{N_r}\left[\frac{p(i,j\|\theta)}{i^2}\right]}{\sum_{i=1}^{N_g}\sum_{j=1}^{N_r} p(i,j\|\theta)}$
Shape	Compactness	Compactness of tumor volume.		$\frac{V}{\sqrt{\pi}A^{\frac{2}{3}}}$
Shape	Spherical disproportion	Sphericity of tumor volume.		$\frac{A}{4\pi R^2}$
First-order statistic	Kurtosis	Existence of extreme values.		$\frac{\frac{1}{N}\sum_{i=1}^{N}(X(i)-\bar{X})^4}{\left(\sqrt{\frac{1}{N}\sum_{i=1}^{N}(X(i)-\bar{X})^2}\right)^2}$
First-order statistic	Median	Median voxel intensity.		$median(X)$
First-order statistic	Minimum	Minimum voxel intensity.		$\min(X)$

Supplementary File 2: R output detailing library version of statistical packages used for analysis.

```
R version 3.1.0 (2014-04-10)
Platform: x86_64-unknown-linux-gnu (64-bit)

locale:
 [1] LC_CTYPE=en_US.UTF-8       LC_NUMERIC=C
 [3] LC_TIME=en_US.UTF-8        LC_COLLATE=en_US.UTF-8
 [5] LC_MONETARY=en_US.UTF-8    LC_MESSAGES=en_US.UTF-8
 [7] LC_PAPER=en_US.UTF-8       LC_NAME=C
 [9] LC_ADDRESS=C               LC_TELEPHONE=C
[11] LC_MEASUREMENT=en_US.UTF-8 LC_IDENTIFICATION=C

attached base packages:
 [1] grid      stats4    parallel  splines   stats     graphics  grDevices
 [8] utils     datasets  methods   base

other attached packages:
 [1] randomForest_4.6-12  kernlab_0.9-23       glmnet_2.0-2
 [4] foreach_1.4.2        Matrix_1.1-4         rmeta_2.16
 [7] km.ci_0.5-2          gplots_2.15.0        pROC_1.7.3
[10] reshape2_1.4.1       caret_6.0-41         ggplot2_1.0.0
[13] lattice_0.20-29      FactoMineR_1.28      RadioGx_1.9
[16] mRMRe_2.0.5          igraph_0.7.1         cgdsr_1.1.33
[19] eisa_1.18.0          isa2_0.3.3           GO.db_3.0.0
[22] RSQLite_1.0.0        DBI_0.3.1            RamiGO_1.12.0
[25] gsubfn_0.6-6         proto_0.3-10         genefu_1.15.1
[28] biomaRt_2.22.0       mclust_4.4           AnnotationDbi_1.28.1
[31] GenomeInfoDb_1.2.3   IRanges_2.0.1        S4Vectors_0.4.0
[34] Biobase_2.26.0       BiocGenerics_0.12.1  survcomp_1.16.0
[37] prodlim_1.5.1        survival_2.37-7      dplyr_0.4.1

loaded via a namespace (and not attached):
 [1] amap_0.8-12          annotate_1.44.0      assertthat_0.1
 [4] bitops_1.0-6         bootstrap_2014.4     BradleyTerry2_1.0-5
 [7] brglm_0.5-9          car_2.0-22           Category_2.32.0
[10] caTools_1.17.1       class_7.3-11         cluster_1.15.3
[13] codetools_0.2-9      colorspace_1.2-4     compiler_3.1.0
[16] digest_0.6.6         e1071_1.6-7          gdata_2.13.3
[19] genefilter_1.48.1    graph_1.44.1         GSEABase_1.28.0
[22] gtable_0.1.2         gtools_3.4.1         iterators_1.0.7
```

```
[25] KernSmooth_2.23-13   labeling_0.3         lava_1.3
[28] lazyeval_0.1.10      leaps_2.9            lme4_1.1-7
[31] magrittr_1.5         MASS_7.3-35          minqa_1.2.4
[34] munsell_0.4.2        nlme_3.1-118         nloptr_1.0.4
[37] nnet_7.3-11          plyr_1.8.1           png_0.1-7
[40] RBGL_1.42.0          RColorBrewer_1.1-2   Rcpp_0.11.3
[43] RCurl_1.95-4.5       RCytoscape_1.16.0    R.methodsS3_1.6.1
[46] RMiscPG_1.0          R.oo_1.18.0          R.utils_1.34.0
[49] scales_0.2.4         scatterplot3d_0.3-35 stringr_0.6.2
[52] SuppDists_1.1-9.1    survivalROC_1.0.3    tcltk_3.1.0
[55] tools_3.1.0          XML_3.98-1.1         XMLRPC_0.3-0
[58] xtable_1.7-4
```

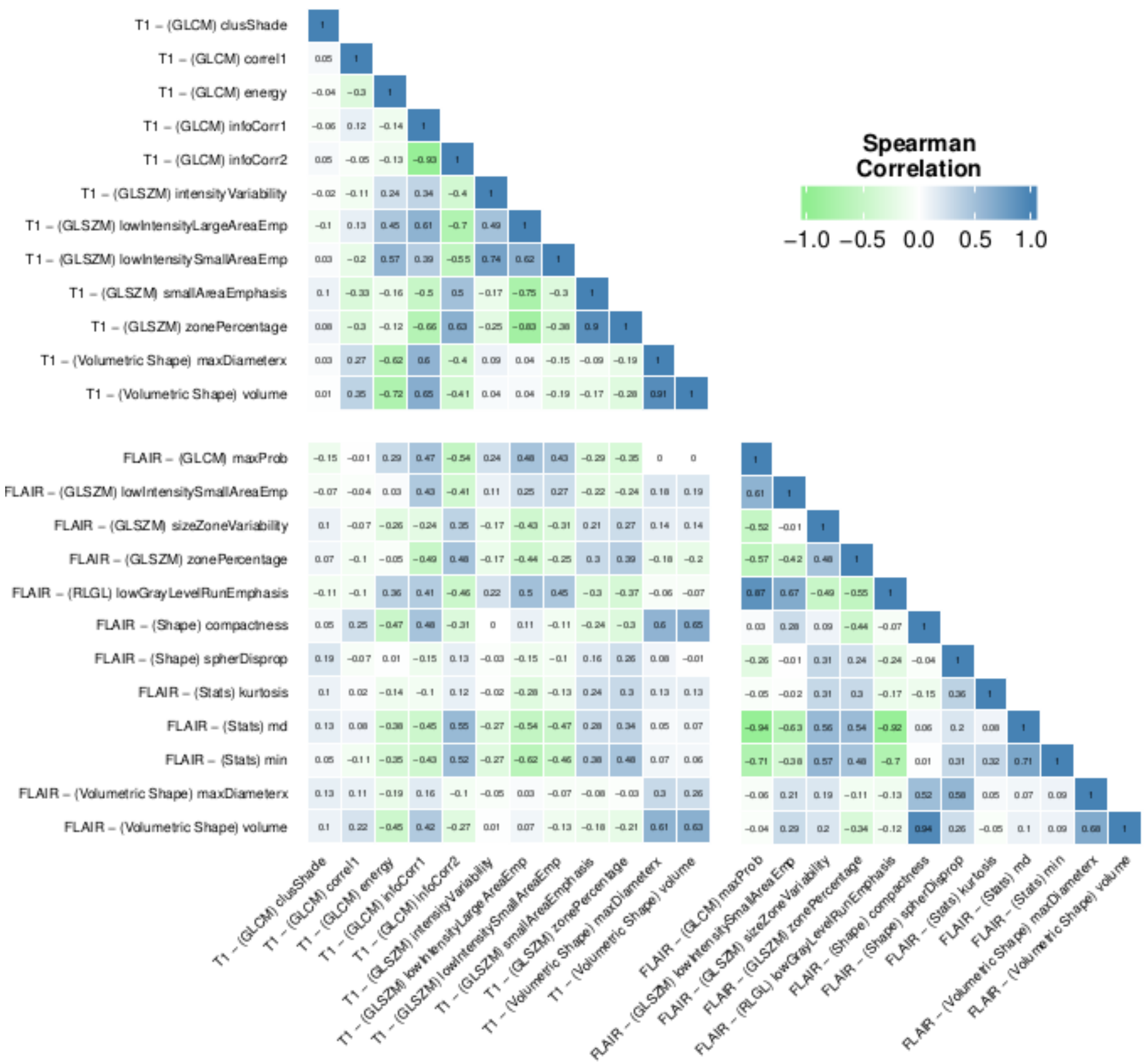

Supplementary Figure 1: Pairwise Spearman rank correlation of all features derived from T1-weighted and FLAIR imaging at baseline. Correlation was generally low indicating independence of individual feature pairs.

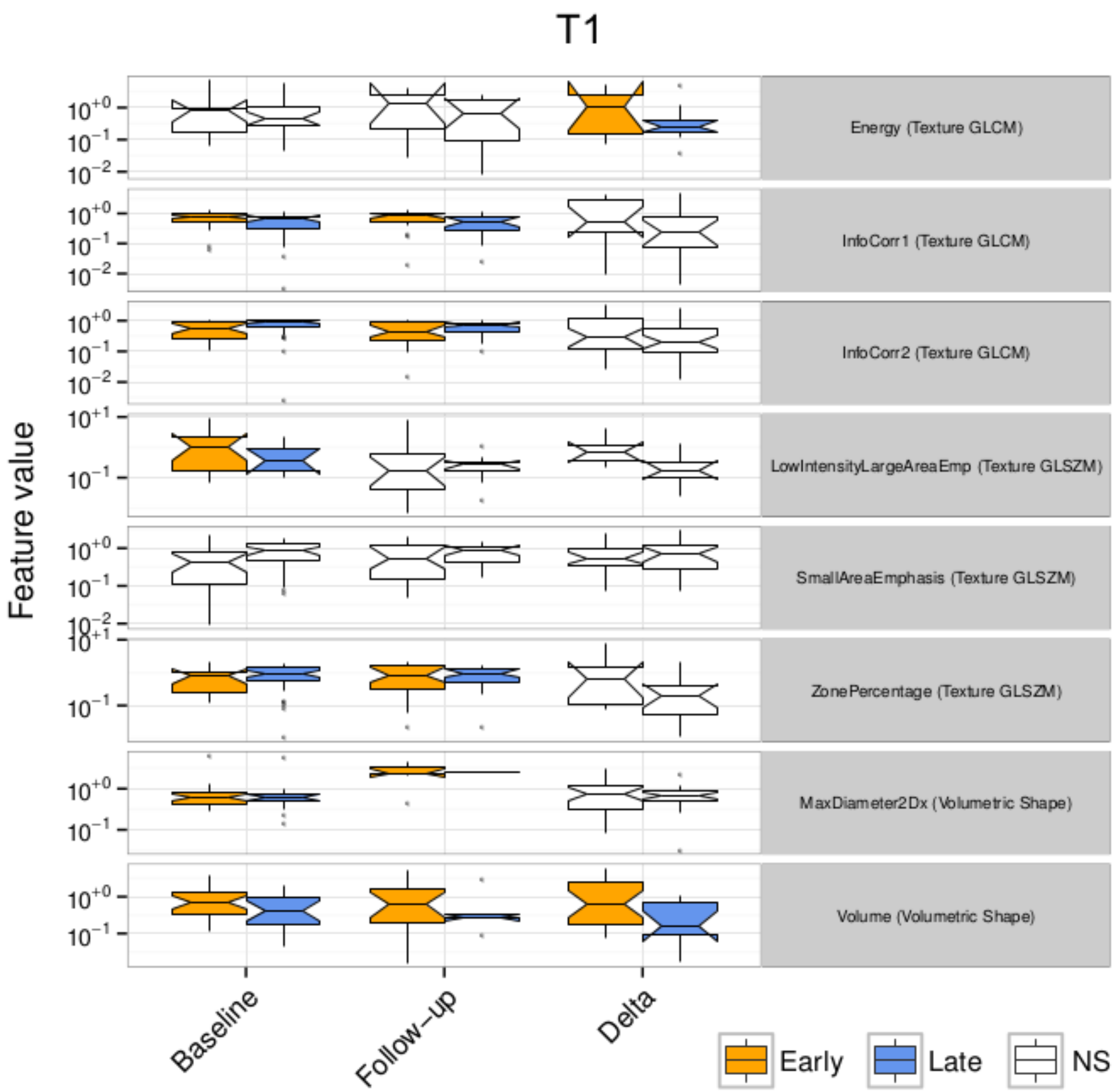

Supplementary Figure 2: Values distribution in early (< 3 months) and late (> 6 months) progressors of selected features (see Fig. 3). Significant differences (Wilcoxon rank-sum test $p < 0.05$) in feature value distribution (displayed as log10 scaled Z-scores) of early versus late progression was observed only for features derived from post-contrast T1-weighted imaging (colored bars). Notably, intra-tumor heterogeneity, as measured by information correlation, was significantly greater for patients progressing early as compared to patients progressing late.

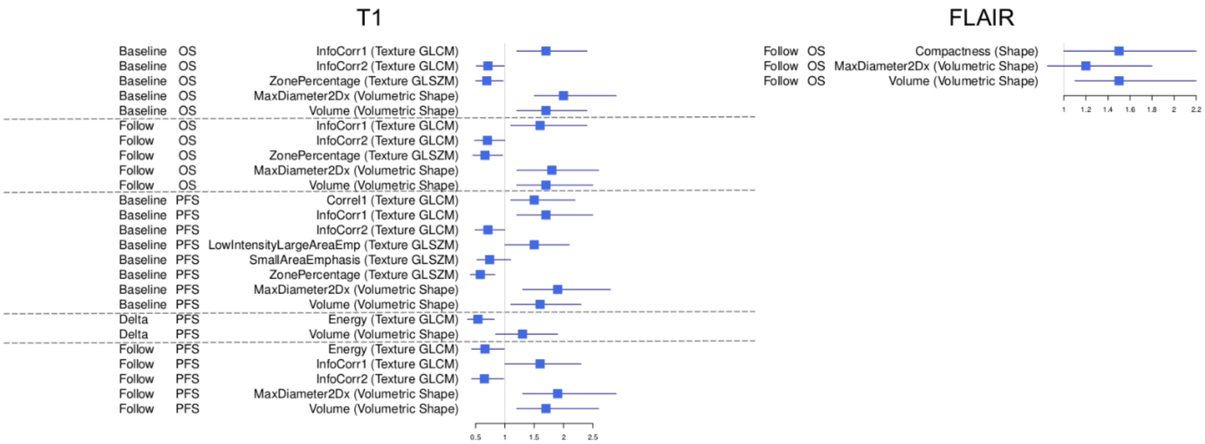

Supplementary Figure 3: Stratification power of radiomic features. Hazard-ratios for overall survival (OS) and progression-free survival (PFS) displayed with 95% confidence intervals of significant prognostic features (see Fig. 3) for baseline and follow-up imaging, as well as for the delta between baseline and follow-up.

Supplementary Table 3: Hazard-ratio (HR) statistics of features that performed significantly for an imaging modality, clinical endpoint, and timepoint (compare Fig. 3). Other abbreviations: *p*=p-value of one-sided t-test, SE=standard error, ci=95% confidence interval.

Modality	Endpoint	Timepoint	Feature	HR	p	SE	ci lower	ci upper
FLAIR	OS	Follow	Shape_compactness	1.5	0.031	0.19	1	2.2
FLAIR	OS	Follow	Volumetric_Shape_maxDiameter2Dx	1.2	0.27	0.19	0.85	1.8
FLAIR	OS	Follow	Volumetric_Shape_volume	1.5	0.024	0.19	1.1	2.2
T1	OS	Baseline	GLCM_infoCorr1	1.7	0.002	0.17	1.2	2.4
T1	OS	Baseline	GLCM_infoCorr2	0.71	0.042	0.17	0.51	0.99
T1	OS	Baseline	GLSZM_zonePercentage	0.69	0.03	0.17	0.5	0.97
T1	OS	Baseline	Volumetric_Shape_maxDiameter2Dx	2	3.4e-05	0.17	1.5	2.9
T1	OS	Baseline	Volumetric_Shape_volume	1.7	0.0012	0.17	1.2	2.4
T1	OS	Follow	GLCM_infoCorr1	1.6	0.015	0.2	1.1	2.4
T1	OS	Follow	GLCM_infoCorr2	0.7	0.062	0.19	0.48	1
T1	OS	Follow	GLSZM_zonePercentage	0.66	0.031	0.19	0.45	0.96
T1	OS	Follow	Volumetric_Shape_maxDiameter2Dx	1.8	0.0037	0.2	1.2	2.6
T1	OS	Follow	Volumetric_Shape_volume	1.7	0.0072	0.2	1.2	2.5
T1	PFS	Baseline	GLCM_correl1	1.5	0.024	0.18	1.1	2.2
T1	PFS	Baseline	GLCM_infoCorr1	1.7	0.0029	0.18	1.2	2.5
T1	PFS	Baseline	GLCM_infoCorr2	0.71	0.056	0.18	0.49	1
T1	PFS	Baseline	GLSZM_lowIntensityLargeAreaEmp	1.5	0.037	0.18	1	2.1
T1	PFS	Baseline	GLSZM_smallAreaEmphasis	0.74	0.092	0.18	0.52	1.1
T1	PFS	Baseline	GLSZM_zonePercentage	0.58	0.0031	0.18	0.41	0.83
T1	PFS	Baseline	Volumetric_Shape_maxDiameter2Dx	1.9	0.00039	0.18	1.3	2.8
T1	PFS	Baseline	Volumetric_Shape_volume	1.6	0.011	0.18	1.1	2.3
T1	PFS	Delta	GLCM_energy	0.54	0.0037	0.21	0.36	0.82
T1	PFS	Delta	Volumetric_Shape_volume	1.3	0.26	0.21	0.84	1.9
T1	PFS	Follow	GLCM_energy	0.66	0.045	0.21	0.43	0.99
T1	PFS	Follow	GLCM_infoCorr1	1.6	0.032	0.21	1	2.3
T1	PFS	Follow	GLCM_infoCorr2	0.65	0.04	0.21	0.43	0.98
T1	PFS	Follow	Volumetric_Shape_maxDiameter2Dx	1.9	0.0024	0.21	1.3	2.9
T1	PFS	Follow	Volumetric_Shape_volume	1.7	0.0083	0.21	1.2	2.6

Supplementary Table 4: Sensitivity and specificity of multivariable overall survival and progression models on validation data reported in Fig. 4.

	One-year Overall Survival	3 months progression	6 months progression	9 months progression
Sensitivity	0.60	0.48	0.70	0.50
Specificity	0.77	0.65	0.69	0.84

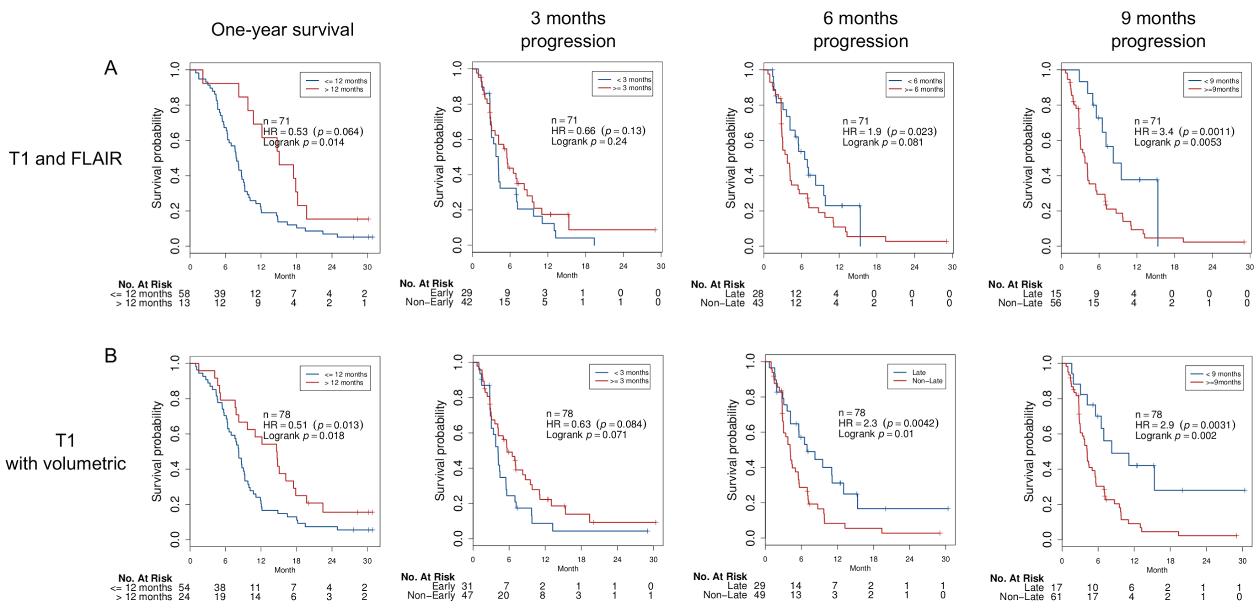

Supplementary Figure 4: Kaplan-Meier estimates of baseline progression and overall survival models. Models included the combination of post-contrast T1-weighted imaging derived features selected from delta as presented in Fig. 4 of the manuscript. In addition, the models here combined **(A)** post-contrast T1-weighted imaging derived and volumetric features **(B)** features derived from both post-contrast T1-weighted and FLAIR imaging. All models have been adjusted for age, sex, and Karnofsky performance status at baseline.